Surface Bonding and Dynamical Behavior of the CH_3SH Molecule on Au(111)

Peter Maksymovych,[†] Dan C. Sorescu,[‡] Dan Dougherty,[†] and John T. Yates, Jr.*[,†]

Surface Science Center, Department of Chemistry, University of Pittsburgh, Pittsburgh, Pennsylvania 15260, and U.S. Department of Energy, National Energy Technology Laboratory, Pittsburgh, Pennsylvania 15236

Received: May 9, 2005

The chemisorption of the undissociated CH_3SH molecule on the Au(111) surface has been studied at 5 K using scanning tunneling microscopy (STM) and density functional theory (DFT) calculations. The molecule was found to adsorb on atop Au sites on the defect-free surface. CH_3SH undergoes hindered rotation about the Au−S bond on the defect-free surface which is seen in STM as a time-averaged 6-fold pattern. The pattern suggests that the potential minima directions occur for the rotating molecule at the six hollow sites surrounding the atop adsorption site. The barrier for rotation, obtained by DFT calculations, is ∼0.1 kcal·mol^{-1}. At low coverages, preferential adsorption occurs at defect sites in the surface, namely, the herringbone "elbows" and random atomic step sites. Molecules adsorbed on these sites do not exhibit rotational freedom.

1. Introduction

Interest in the surface chemistry of alkanethiols has been stimulated by their application for the growth of self-assembled monolayers (SAMs).[1] These layers have applications in the field of molecular electronics,[2] lubrication,[3] lithography,[4] and biochemical surface functionalization.[5]

The surface bonding of alkanethiols and the dissociation of the S−H bond have remained controversial. A number of studies have assigned CH_3SH adsorbed on Au(111) as a dissociated methanethiolate species, CH_3S.[6] Initially, the adsorption site for CH_3S was assigned as the bridge or hollow position on the surface.[7,8] Recent photoelectron diffraction studies suggested that the CH_3S species binds to atop Au atom sites.[9]

However, the CH_3SH molecule has recently been shown to chemisorb on the reconstructed Au(111) surface without S−H bond dissociation.[10] In this study, we probe the site location for CH_3SH bonding, finding that the molecule occupies an atop Au site on the defect-free Au(111) surface.

To the best of our knowledge, there is only one theoretical study in which the binding site and configuration of the undissociated CH_3SH species was predicted.[11] The CH_3SH species was theoretically found to lie nearly parallel to the surface with the S atom binding on the Au atom atop site.[11]

CH_3SH is a natural candidate molecule for the characterization of the HS−Au bond because it is the shortest alkanethiol and its bonding to the surface occurs primarily through the SH group in contrast to longer alkanethiol molecules, where the interaction of the alkane chain with the surface is significant at low coverages.

2. Experimental Methods

Scanning tunneling microscopy experiments were conducted with a commercial low-temperature scanning tunneling microscope (Omicron Nanotechnology) operating in an ultrahigh vacuum (UHV) chamber (background pressure $<5.0 \times 10^{-11}$ Torr). The Au(111) crystal was cleaned by Ar^+ sputtering and annealing to 773 K. CH_3SH was deposited on the surface through an effusive beam doser while the crystal was in the scanning tunneling microscopy imaging position at <10 K. The STM images presented here were taken at a temperature of ∼5 K or at 77 K where specified. The scanner calibration was verified by measuring the lattice constant of the Au(111) surface (average distance measured 2.81 ± 0.07 Å, bulk lattice constant 2.88 Å). All of the STM images have been minimally processed by plane subtraction and smoothing. Voltage pulsing with the STM tip was used to move CH_3SH molecules, and the typical pulsing conditions were $V = -0.6$ V and $t = 10$ ms.

3. Theoretical Method

The density functional theory (DFT) calculations were done in the slab model using the Vienna ab initio simulation package (VASP).[12] The electron−ion interaction has been described using the projector augmented wave (PAW) method of Blöchl[13] in the implementation of Kresse and Joubert.[14] All calculations have been done using the PW91 generalized gradient approximation (GGA) of Perdew et al.[15] The k points were obtained from the Monkhorst−Pack scheme,[16] with a cutoff energy of 400 eV. Electron smearing was employed via the Methfessel−Paxton technique,[17] with a smearing width consistent with $\sigma = 0.1$ eV, to minimize the errors in the Hellmann−Feynman forces due to the entropic contribution to the electronic free energy.[12]

All energies were extrapolated to $T = 0$ K. The value of E_{cut} and the k-point grid were chosen to ensure the convergence of energies and structures. In particular, using an $8 \times 8 \times 8$ k-point mesh for the bulk unit cell of Au, we obtained a lattice dimension of $a_{calcd} = 4.1744$ Å and a cohesive energy of $E_{coh,calcd} = 3.21$ eV. These values agree well with the corresponding experimental data of $a_{exptl} = 4.078$ Å and $E_{coh} = 3.81$ eV as well as with the values determined in other theoretical studies.[7,11]

An equally good representation has been obtained for the geometric parameters of the isolated CH_3SH molecule. On the basis of optimizations performed in a cubic box of size 12 Å, we have determined equilibrium bond lengths of r(S−C) = 1.820 Å, r(S−H) = 1.349 Å, and r(C−H) = 1.095−1.096 Å and a bond angle of θ(C−S−H) = 96.8°. These values are in close agreement with the experimental values reported in ref

* Corresponding author. E-mail: jyates@pitt.edu.
[†] University of Pittsburgh.
[‡] U.S. Department of Energy.

10.1021/jp058154u CCC: $30.25
Published on Web 10/05/2005

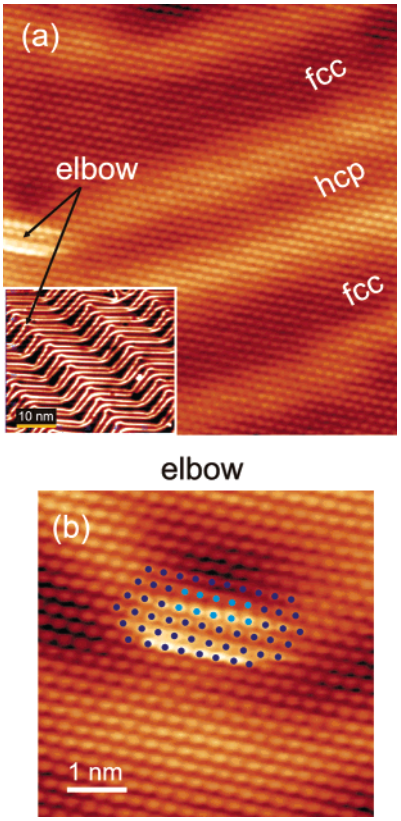

Figure 1. Atomically resolved STM images at 5 K of the clean Au-(111)-22×√3 reconstructed surface ($U = -0.014$ V, $I = 0.05$ nA). (a) Low-magnification image showing uniaxial domains of fcc and hcp vertical stacking. The inset shows a large-scale STM image of the herringbone reconstruction. (b) High-magnification image of the elbow region. The blue circles mark the apparent centers of the underlying Au atoms. The light blue color corresponds to the coordinatively unsaturated atoms, which exhibit increased reactivity.

18: $r_{exptl}(S-C) = 1.819$ Å, $r_{exptl}(S-H) = 1.340$ Å, $r_{exptl}(C-H) = 1.090$ Å, and $\theta_{exptl}(C-S-H) = 96.5°$.

4. Results

4.1. STM Study of the Clean Au(111) Surface. The "herringbone" reconstruction occurs naturally for the atomically clean Au(111) surface to allow the surface layer to have a more close-packed structure than the bulk-terminated (111) plane.[19] The process leading to the reconstruction can be described as the insertion of 1 extra Au atom for every 22 atoms along the close-packed [$1\bar{1}0$] direction.[20] To accommodate the extra atom, slight buckling of the Au surface layer occurs, and the resulting Au surface is comprised of a periodic sequence of alternating uniaxial domains of regular face-centered cubic (fcc) and hexagonal close-packed (hcp) vertical stacking. The domain boundaries are discommensuration lines, where the stacking is intermediate between fcc and hcp.[19]

Figure 1a shows an STM topograph of a clean Au(111) surface. The discommensuration lines appear as bright stripes, the fcc domains as broad, dark regions, and the hcp domains as narrow, dark regions. The apparent height difference between the hcp and fcc stacked domains and the faulted stacked domains is ~0.2 Å. The periodicity in the [$1\bar{1}0$] direction is ~63 Å.

On a larger scale, the [$1\bar{1}0$] direction, along which the compression occurs, is periodically rotated by 120° (inset of Figure 1a) to an equivalent one due to the 3-fold symmetry of the surface. This was shown to be due to long-range elastic forces on the Au(111) surface.[21] The period of rotation is ~150 Å, and the resulting pattern is called the herringbone reconstruction. The surface region at the point of rotation is usually referred to as an elbow site, and it has a single missing Au atom. The defective structure of the elbow site makes it a preferential nucleation center in heteroepitaxy of metals, such as Fe, Co, and Ni.[22]

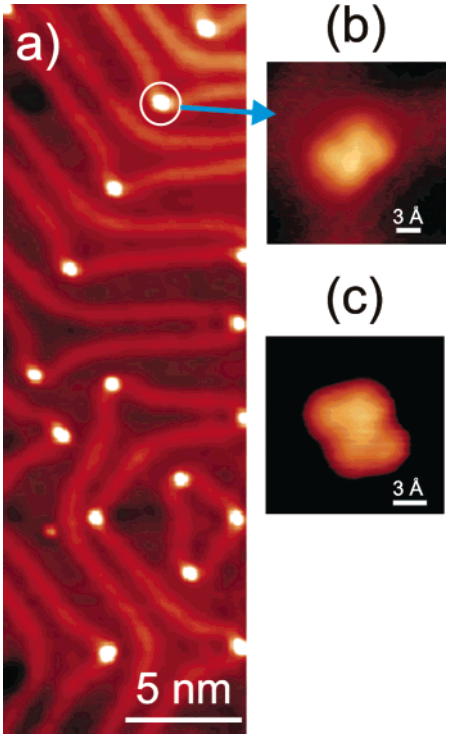

Figure 2. STM image at 77 K of the surface with 0.01 ML of CH_3SH showing preferential adsorption of CH_3SH on the elbow sites ($U = -0.3$ V, $I = 0.04$ nA). (a) The molecules are seen as bright protrusions located on the elbow sites. The molecules adsorb on one of the two discommensuration lines in the elbow region. (b and c) Representative high-resolution images of the protrusions at the elbow sites. A pair of two-lobed features is seen at every elbow. Each two-lobed feature corresponds to a CH_3SH molecule.

An atomically resolved STM image of the elbow site is shown in Figure 1b. Although both discommensuration lines turn by 120° at the elbow, only one line contains a missing Au atom. This is shown by a set of dots superimposed onto the positions of the Au atoms in Figure 1b. The missing Au atom is evident, when comparing the coordination of the light blue dots to that of the dark blue dots.

4.2. Adsorption of CH_3SH on Au(111) at Low Coverage—Selection of Defect Sites. We first identify the most reactive sites for CH_3SH adsorption on the reconstructed Au(111) surface.

A small amount of CH_3SH was dosed on a clean Au(111) surface at 10 K. The surface was then heated to ~80 K and cooled back to 77 or 5 K for imaging by STM. Heating to 80 K is required to allow CH_3SH molecules to probe the potential energy landscape of the surface by diffusion. From our experience, diffusion of isolated CH_3SH molecules on the nondefective surface becomes noticeable in STM at >70 K. CH_3SH dissociation will not occur at 80 K.[10]

A large-scale image in Figure 2a was obtained for a CH_3SH coverage of <0.01 ML.[23] In comparison to the clean surface (Figure 1), an array of bright protrusions due to CH_3SH adsorbate species occurred at the elbow sites, each of which has a missing Au atom.

High-resolution scans reveal that every protrusion on the elbow is composed of two or very rarely three identical features

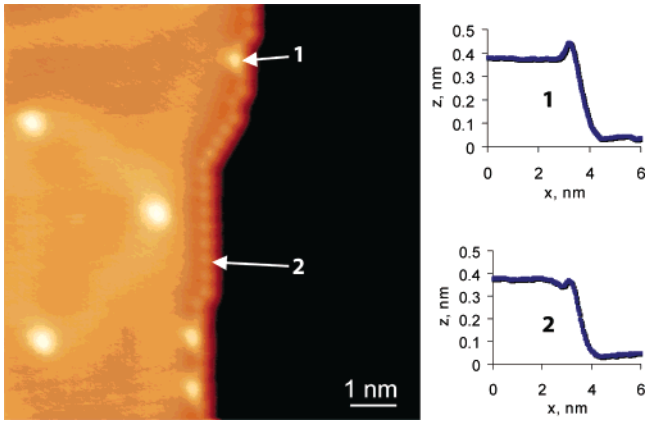

Figure 3. Preferential adsorption of CH_3SH to a high local coverage at the step sites. Two kinds of molecular species are seen: species-1, CH_3SH on top of the step; species-2, CH_3SH at the base of the step. The corresponding STM line profiles are shown for both species.

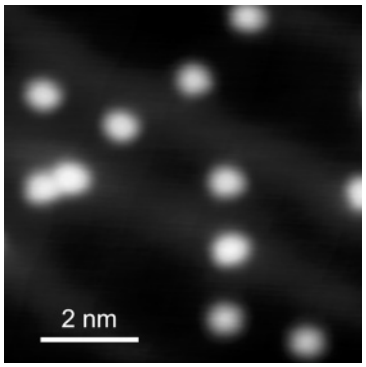

Figure 4. Low-resolution STM image of CH_3SH molecules at 5 K on the defect-free regions of the surface ($U = -0.16$ V, $I = 0.2$ nA).

(Figure 2b and c). Each feature has an elliptical shape with two lobes separated by a node in the middle (hereafter two-lobed shape). The full width at half-maximum (fwhm) of the line profile along the longer axis of the ellipse is 7 Å. We believe the two-lobed feature represents a single adsorbed CH_3SH molecule and observe that often several species are located at the elbow sites.

In addition to adsorption at the defective elbow site, it is also seen (Figure 3) that CH_3SH adsorption occurs to a high local coverage at the atomic step sites. Two types of features are observed, a bright protrusion on top of the step (1) and a less bright protrusion at the base of the step (2). The location of the features relative to the step is assigned on the basis of the line scans over each of these features, which are shown in Figure 3 in the insets. The two features do not coexist; that is, the 1-D chain of species-2 molecules is terminated where species-1 molecules are observed; this might be due to steric repulsion between CH_3SH molecules.

In summary, at 80 K, the mobile CH_3SH molecules are observed to preferentially select two types of sites at low coverage. These are the elbow sites containing a missing Au atom and the atomic step sites present at random steps on the surface.

4.3. Adsorption of CH_3SH on Defect-Free Sites of Au(111)—Observation of Hindered Rotation of CH_3SH at 5 K. The occupancy of sites on the defect-free surface can be observed in STM by raising the coverage of CH_3SH.

Figure 4 shows an STM image obtained after dosing ~0.05 ML of CH_3SH on a clean Au(111) surface at <10 K. The molecules are imaged as nearly round protrusions 8 Å in diameter and 0.9 ± 0.1 Å in height. Some molecules look brighter in the image because they are adsorbed on topographically higher discommensuration lines.

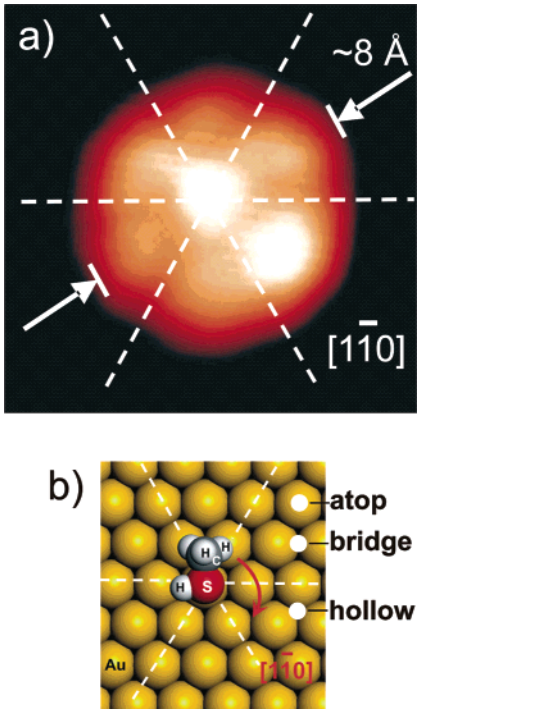

Figure 5. (a) High-resolution STM image at 5 K of a single rotating CH_3SH molecule on the nondefective surface in the shape of a flower with six petals ($U = -0.01$ V, $I = 0.04$ nA) The dashed lines correspond to the close-packed crystallographic directions determined from atomically resolved STM images of the Au lattice in the vicinity of the molecule. (b) A schematic model of the adsorption geometry inferred from the STM image.

The diameter of the CH_3SH molecules as seen by STM is about 2 times as large as the effective diameter of the molecule, which is defined as the maximum linear dimension of the CH_3SH space-filling model. To understand this discrepancy, high-resolution STM images were obtained.

An example of a high-resolution image is shown in Figure 5, where the resolution was improved by pulsing the STM tip with ±10 V pulses and scanning at a lower bias.

As seen in Figure 5a, the CH_3SH image exhibits an apparent flower shape with six petals around a bright dot in the center. The average apparent diameter of the flower, along the petal—center—petal line, is 8 Å, which is identical to the diameter of the molecular image seen at a lower resolution in Figure 4.

The flower-shaped appearance of the CH_3SH image can be explained by assuming that the molecule undergoes hindered rotation on the surface. In this case, the STM image taken at the time scale of seconds represents a time-averaged picture of the rotating molecule. The azimuthal directions of the petals correspond to the potential minima along the rotational coordinate; the residence time of the molecule is longer at each of the six potential minima. Conversely, the rotation potential maxima correspond to the close-packed Au—Au azimuths shown by dashed lines in Figure 5. Similar rotational patterns were seen for a chlorinated benzenethiol molecule chemisorbed on Cu(111).[24]

Direct evidence for the rotation of the molecule was obtained by moving two CH_3SH molecules together on the surface. This is illustrated in Figure 6.

In Figure 6a, all of the molecular images have a flower shape due to rotation. The STM tip was positioned above molecule

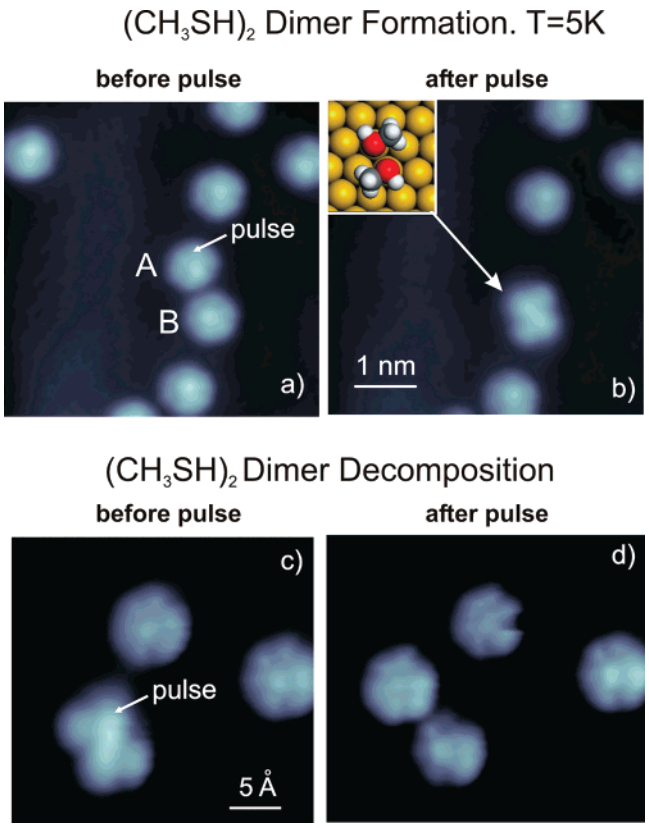

Figure 6. Direct evidence for steric hindrance to the rotation of CH_3SH molecules on Au(111) at 5 K ($U = -1$ mV, $I = 0.05$ nA). (a) STM image of rotating molecules before the manipulation. The arrow shows the position where a pulse of -0.6 V was applied in order to move molecule A toward molecule B. (b) Molecular rotation stops as a result of the proximity of two molecules. Molecules A and B form a zigzag-shaped dimer. The inset of Figure 6b shows a possible $(CH_3SH)_2$ head-to-tail dimer model. (c) A voltage pulse of $+0.6$ V was applied to dissociate the CH_3SH dimer. (d) After dimer dissociation, both CH_3SH molecules undergo hindered rotation, indicating that the dimerization does not involve the formation of chemical bonds between CH_3SH molecules.

A, and a pulse of -0.6 V was applied to move it toward molecule B. The result is shown in Figure 6b, where molecules A and B form a single entity, which has a zigzag shape and is composed of two identical two-lobed shapes in an antiparallel orientation. Each two-lobed shape has a node separating two lobes of slightly different size. The geometry of the zigzag species implies that it is a dimer of two CH_3SH molecules, where the two-lobed shapes correspond to individual CH_3SH molecules. A possible model for the CH_3SH dimer corresponding to the STM image is shown in the inset of Figure 6b.

The rotation of individual molecules in the dimer will be unfavorable due to steric hindrance, which is consistent with the observations. The rotational motion is restored when the molecules are moved apart by an STM pulse. This is illustrated in Figure 6c and d. This also implies that CH_3SH dimerization does not involve the formation of chemical bonds between CH_3SH adsorbate molecules.

4.4. Atomic Site Location for Chemisorption. The 6-fold symmetry of the flower shape of the rotating molecule (Figure 5a) implies that there are six equivalent orientations of the molecule around its center of rotation, which requires the adsorption site of the molecule to have 6-fold symmetry in the topmost surface layer. Since the length of the C−S bond (∼1.8 Å) is smaller than the Au lattice constant (∼2.8 Å), only the locations of the nearest-neighbor atoms surrounding a possible adsorption site on the Au(111) surface will have a strong effect on determining the symmetry of the rotational pattern of the CH_3SH molecule.

TABLE 1: Calculated Equilibrium Distances (Å) and Adsorption Energies for CH_3SH Adsorbed on a Au(111) Surface at Different Surface Sites

configuration	r(Au−S)[a]	r(S−C)	r(S−H)	E_{ads}, kcal/mol
gas phase		1.821	1.350	
top	2.668	1.822	1.352	**8.6**
fcc	3.303	1.824	1.352	2.9
hc[	3.472	1.825	1.352	2.7

[a] r(Au−S) is the shortest distance from the S to the Au atoms in the first layer.

The only surface site with the 6-fold symmetry in the topmost surface layer is the atop site, which is surrounded by six hollow sites and six neighbor atoms (Figure 5b). The hcp and fcc hollow sites have a 3-fold symmetry, and the bridge site has a 2-fold symmetry in the topmost layer. Thus, we assign the atop site as the preferential adsorption site for the CH_3SH molecule on the defect-free Au(111) surface.

In Figure 5a, the dashed lines superimposed on the STM image of the CH_3SH molecule correspond to the close-packed directions on the Au(111) surface, inferred from atomically resolved STM images of the surface area around the molecule. The petals of the flower shape, which correspond to the preferential direction of the molecule along its rotational coordinate, are seen to be located between these lines. This means that the molecule during its rotation is preferentially oriented toward the hollow sites around the Au atom on which the molecule is adsorbed.

5. Discussion

To verify the assignment of the adsorption site based on the STM measurements and to estimate the rotational barrier of CH_3SH on the defect-free Au(111) surface, we have carried out DFT slab calculations with CH_3SH adsorbed on the unreconstructed Au(111) surface.

5.1. Adsorption Site by DFT Calculations. Several adsorption configurations of the CH_3SH molecule on the Au(111) unreconstructed surface have been studied using a 3×3 supercell model with four Au layers. The two top layers of the slab model together with the adsorbed molecule were allowed to optimize, while the two bottom layers of the slab were frozen in the bulk optimized configuration.

Table 1 (Figure 7) summarizes the binding energies and representative geometric parameters obtained for different adsorption sites of the CH_3SH molecule. The adsorption sites listed in Table 1 refer to the position of the S atom of the CH_3SH molecule on the surface. According to these data, the atop adsorption configuration (Figure 7) is the most stable, because its binding energy is nearly 3 times as high as that of the hollow fcc or hollow hcp configurations. This is in good agreement with the STM results, where the absolute majority of the molecules exhibit a 6-fold symmetrical pattern due to molecular rotation, which, as described in section 4.4, implies bonding of the molecule to the atop site. We have also analyzed the case when adsorption takes place at the bridge site, but the corresponding configuration was found to be unstable, and the molecule moved to the atop site during energy minimization.

In the atop configuration, the molecule is tilted toward the surface (Au−S−C angle of 108°) and the Au−S bond length is about 2.664 Å (Figure 7). The S−C molecular axis is in a plane bisecting the 60° angle formed by the two surface Au

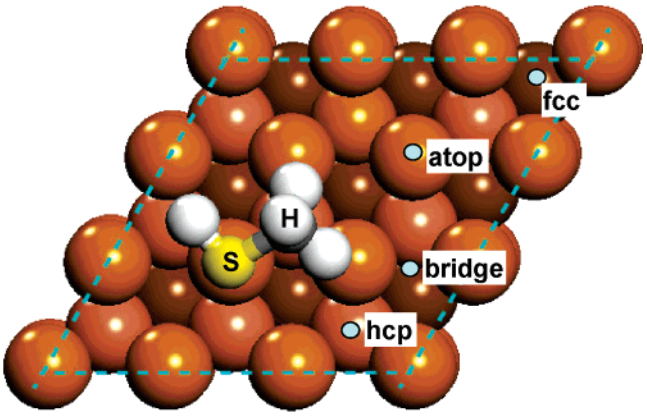

Figure 7. DFT optimized adsorption geometry of CH_3SH on an unreconstructed Au(111) surface. The molecule adsorbs with the SH group on top of the Au atom and the CH_3 group above the hollow site. Table 1 lists the adsorption geometries and energies for the possible adsorption sites on the surface.

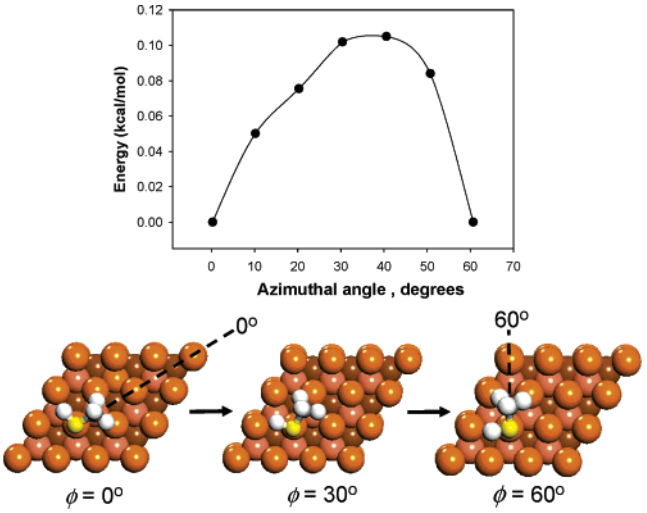

Figure 8. Minimum energy path for the rotation of a CH_3SH molecule around the S−Au bond as a function of the azimuthal angle (ϕ) . The zero point corresponds to the geometry in Figure 7.

atoms nearest to the Au atom on which the molecule is adsorbed. The methyl group is positioned above the hollow site (Figure 7). This is also consistent with the STM image (Figure 5a) of the CH_3SH molecule, where the petals of the flower shape have the same orientation.

In summary, the CH_3SH molecule preferentially binds to the atop adsorption site with the SH group directly above the Au atom and the methyl group directed toward the neighbor hollow site. In the flower-shaped STM image of the rotating CH_3SH molecule, the petals are due to the CH_3 groups and a bright feature in the center marks the position of the SH group.

5.2. Rotational Behavior and Estimate of Barrier Height. The minimum energy path for CH_3SH rotation around the S−Au bond between successive equilibrium configurations (see Figure 8) was determined by use of the nudged elastic band (NEB) method of Jónsson and co-workers.[25] In this approach, the reaction path is "discretized", with the discrete configurations, or images, between the potential minima being connected by elastic springs to prevent the images from sliding to the minima in the optimization. The energies of the intermediate states along the reaction path are simultaneously minimized, but the atomic motion is restricted to a hyperplane perpendicular to the reaction path. Specifically, we have used a set of five images distributed in increments of 10° among the equilibrium configurations. The results plotted in Figure 8 represent the minimum energy path versus the azimuthal angle of rotation (ϕ). In the initial and final configurations, the CH_3 group is located above the hollow hcp or fcc site, respectively. In the least favorable orientation, the CH_3 group is located in the direction of the near-neighbor Au atom ($\phi = 30°$ in Figure 8). The maximum barrier height for rotation is ~0.1 kcal·mol^{-1}. The small calculated energy of the rotational barrier is at the limit of the accuracy of DFT, so we assign it as the upper limit of the true barrier.

The asymmetry of the potential energy curve around the direction to the near-neighbor Au atom ($\phi = 30°$) is due to the difference in the surface structure when approaching this direction from the side of the fcc site and the hcp site.

To validate the possibility of observing the rotational motion of a molecule at 5 K, we estimate the rate of rotation from the standard Arrhenius equation

$$\text{rate} = A \exp\left(\frac{-E_{\text{rot}}}{RT}\right)$$

using 0.1 kcal·mol^{-1} for the rotational barrier (E_{rot}) and a conservative estimate of 10^{11} s^{-1} for the preexponential factor (A). This yields a rate of ~10^7 hops/s at 5 K. Since one full rotation takes six hops, the molecule makes ~10^6 full rotations per second at this temperature.

Thus, the appearance of the full rotational pattern in the STM image at 5 K is plausible, given that the average time of an STM measurement of a single molecule is 10 s. Moreover, the electric field due to the proximity of the STM tip may further decrease the rotational barrier, causing more rotations per second during the experimental imaging.

5.3. CH_3SH Molecules Chemisorbed on Step and Elbow Sites. The apparent shape of the two-lobed features located on the elbow sites (Figure 2b and c) is very similar to the components of the CH_3SH dimer image (Figure 6b and c) formed by moving two molecules close to each other. This allows us to assign the elbow features to CH_3SH molecules.

On average, two molecules occupy the elbow site; however, at very low coverage, a single two-lobed shape can be observed at the elbow site (not shown). Observation of a single two-lobed shape of the molecule at the elbow site, as opposed to the six-petal image on the defect-free area, implies that the molecules at the elbow do not rotate. This is consistent with the higher binding energy of the molecules at the elbow sites, as discussed above (see section 4.2). Corollary temperature programmed desorption measurements on Au(111) (purposely made defective by Ar^+ bombardment) have also shown that defective sites cause an increase in the CH_3SH desorption temperature.[10]

Lack of rotation is also observed for the molecules adsorbed on the step sites (Figure 3), because their apparent diameter (4 Å) is significantly smaller than that of the molecular images on the defect-free surface (8 Å). The step sites, in addition to binding molecules more strongly, have a broken symmetry in the direction normal to the step edge, which should produce an even higher barrier of rotation at these sites.

6. Summary of Results

The adsorption site and the dynamics of rotational motion of chemisorbed CH_3SH species at low coverages on Au(111) have been studied using STM and DFT calculations. The following results have been obtained:

(1) The undissociated CH_3SH molecule binds to an atop Au(111) site on a defect-free Au(111) surface. The calculated binding energy is 8.6 kcal·mol^{-1} at this site.

(2) The isolated molecule undergoes hindered rotation at 5 K on this site; an upper bound of ~0.1 kcal·mol^{-1} has been calculated for the rotational barrier. The potential minima along the rotational coordinate occur in the direction of the six hollow sites around the Au adsorption site, as indicated by the STM measurements and by DFT calculations.

(3) Rotational motion of chemisorbed CH_3SH is impeded by the presence of a neighbor CH_3SH molecule, which forms a head-to-tail dimer, $(CH_3SH)_2$, at 5 K. Dimers can be formed or broken by manipulating molecules with the STM tip.

(4) Preferential binding of CH_3SH to defect sites on the surface has been observed during the first stages of adsorption at 80 K. These minority sites involve missing Au atoms at the elbows of the herringbone reconstruction as well as random atomic steps on the surface.

(5) CH_3SH does not exhibit rotational freedom at 5 K when adsorbed at random step defect or vacancy defect sites present at the herringbone elbows.

Acknowledgment. We thank the W. M. Keck Foundation for support of this work in the W. M. Keck Center for Molecular Electronics, located in the Surface Science Center. We also thank NEDO (Japan) for financial support.

References and Notes

(1) Kato, H. S.; Noh, J.; Hara, M.; Kawai, M. *J. Phys. Chem. B* **2002**, *106*, 9655.

(2) Joachim, C.; Gimzewski, J. K.; Aviram, A. *Nature* **2000**, *408*, 541.

(3) Joyce, S. A.; Thomas, R. C.; Houston, J. E.; Michalske, T. A.; Crooks, R. M. *Phys. Rev. Lett.* **1992**, *68*, 2790.

(4) Liu, G.-Y.; Xu, S.; Qian, Y. *Acc. Chem. Res.* **2000**, *33*, 457.

(5) Motesharei, K.; Myles, D. C. *J. Am. Chem. Soc.* **1998**, *120*, 7328.

(6) Liu, G.; Rodriguez, J. A.; Dvorak, J.; Hrbek, J.; Jirsak, T. *Surf. Sci.* **2002**, *505*, 295.

(7) Yourdshahyan, Y.; Rappe, A. M. *J. Chem. Phys.* **2002**, *117*, 825.

(8) Renzi, V.-D.; Felice, R.-D.; Marchetto, D.; Biagi, R.; Pennino, U.-d.; Selloni, A. *J. Phys. Chem. B* **2004**, *108*, 16.

(9) Kondoh, H.; Kodama, C.; Sumida, H.; Nozoye, H. *J. Chem. Phys.* **1999**, *111*, 1175.

(10) Rzeźnicka, I. I.; Lee J.; Maksymovych, P.; Yates, J. T., Jr. *J. Phys. Chem. B* **2005**, *109*, 15992.

(11) Grönbeck, H.; Curioni, A.; Andreoni, W. *J. Am. Chem. Soc.* **2000**, *122*, 3839.

(12) Kresse, G.; Furthmüller, J. *Phys. Rev. B* **1996**, *54*, 11169.

(13) Blöchl, P. E. *Phys. Rev. B* **1994**, *50*, 17953.

(14) Kresse, G.; Joubert, D. *Phys. Rev. B* **1999**, *59*, 1758.

(15) Perdew, J. P.; Wang, Y. *Phys. Rev. B* **1992**, *45*, 13244.

(16) Monkhorst, H. J.; Pack, J. D. *Phys. Rev. B* **1976**, *13*, 5188.

(17) Methfessel, M.; Paxton, A. T. *Phys. Rev. B* **1989**, *40*, 3616.

(18) *CRC Handbook of Chemistry and Physics*, 81st ed.; Lide, D. R., Ed.; CRC Press: Boca Raton, FL, 2001.

(19) Barth, J. V.; Brune, H.; Ertl, G.; Behm, R. J. *Phys. Rev. B* **1990**, *42*, 9307.

(20) Goyhenex, C.; Bulou, H. *Phys. Rev. B.* **2001**, *63*, 235404.

(21) Bach, C. E.; Giesen, M.; Ibach, H.; Einstein, T. L. *Phys. Rev. Lett.* **1997**, *78*, 4225.

(22) Meyer, J. A.; Baikie, I. D.; Kopatzki, E.; Behm, R. J. *Surf. Sci. Lett.* **1996**, *365*, L647.

(23) According to our data, the CH_3SH monolayer corresponds to a coverage of ~265 molecules per 100 × 100 Å^2 area on the surface.

(24) Rao, B. V.; Kwon, K.-Y.; Liu, A.; Bartels, L. *J. Chem. Phys.* **2003**, *119*, 10879.

(25) (a) Mills G.; Jónsson, H. *Phys. Rev. Lett.* **1994**, *72*, 1124. (b) Mills, G.; Jónsson, H.; Schenter, G. K. *Surf. Sci.* **1995**, *324*, 305. (c) Jónsson, H.; Mills, G.; Jacobsen, K. W. Nudged elastic band method for finding minimum energy paths of transitions. In *Classical Quantum Dynamics in Condensed Phase Simulations*; Berne, B. J., Ciccotti, G., Coker, D. F., Eds.; World Scientific: 1998; p 385.